

Extinction coefficient imaging of turbid media using dual structured laser illumination planar imaging

Elias Kristensson,* Edouard Berrocal, and Marcus Aldén

Department of Physics, Combustion Physics, Lund University, Box 118, S-221 00 Lund, Sweden

*Corresponding author: elias.kristensson@forbrf.lth.se

Received January 27, 2011; revised March 30, 2011; accepted March 31, 2011;

posted March 31, 2011 (Doc. ID 141672); published April 28, 2011

We demonstrate a technique, named dual structured laser illumination planar imaging (SLIPI), capable of acquiring depth-resolved images of the extinction coefficient. This is achieved by first suppressing the multiply scattered light intensity and then measuring the intensity reduction caused by signal attenuation between two laser sheets separated by Δz mm. Unlike other methods also able to measure this quantity, the presented approach is based solely on side-scattering detection. The main advantages of dual SLIPI is that it accounts for multiple scattering, provides two-dimensional information, and can be applied on inhomogeneous media. © 2011 Optical Society of America

OCIS codes: 110.0113, 290.4210, 290.2200.

The extinction coefficient is one of the most important optical properties for the characterization of an inhomogeneous turbid medium. It describes the probability of light-matter interaction per unit distance and equals the sum of the scattering and absorption coefficients. Numerous methods to measure this quantity can be found in the literature, such as time-gated transmission measurements [1], time resolved backscattering and Raman lidar [2], side-scattering detection in combination with measuring transmission [3], and extinction tomography [4]. Some of these examples are restricted to homogeneous volumes, while others can measure the extinction coefficient resolved in either one or two dimensions. A common obstacle when probing turbid media is the successive light scattering events known as multiple scattering. The direct consequence of detecting these undesired photons is an underestimation of the extinction coefficient [1]. In this Letter we demonstrate for the first time, to the best of our knowledge, a technique based solely on side scattering to acquire depth-resolved images of the extinction coefficient where uncertainties introduced by the detection of multiple light scattering are strongly reduced.

Laser sheet imaging is a common approach used to record side-scattered light in dilute media [5]. When applied on more turbid samples, errors in the measurement are introduced by the detection of multiply scattered light. In 2008, a technique—structured laser illumination planar imaging (SLIPI)—capable of diminishing this unwanted contribution of light was demonstrated [6], and its suppression capabilities were investigated quantitatively by Kristensson *et al.* [7]. SLIPI combines laser sheet imaging and structured illumination [8] and consists of superimposing a sinusoidal pattern on the incident laser sheet. When photons are multiply scattered, they lose this structural information and will instead appear as a diffuse background on the recorded image. To extract the singly scattered photons, which are represented by the amplitude of the modulation, three images are required between which the phase of the sinusoidal pattern is shifted $2\pi/3$. The contribution of singly scattered light is then obtained by calculating the rms of the images [8].

Based on SLIPI, the effect of signal attenuation between two laser sheets is measured here, allowing the

average extinction coefficient to be calculated using the Beer–Lambert law. The proposed technique, named dual SLIPI, simultaneously views the sample from both sides of the laser sheet and takes advantage of the symmetrical scattering properties of light (valid for spherical particles or random scattering media) to allow inhomogeneous media to be probed.

Figure 1 shows a top view of the optical arrangement in which two cameras, positioned at $+90^\circ$ and -90° , record the scattered light. To explain the method in detail, one can assume a scattering sample being illuminated with a one-dimensional laser beam that propagates along the x axis with an initial intensity of I_0 . Equations (1) and (2) describe the singly scattered light intensity recorded by each camera at an arbitrary point along the initial direction of the laser beam ($x = x'$):

$$I_1^1(x') = C_1 \cdot S \cdot I_0 \cdot \exp\left(-\int_0^{x'} \mu_e(x, z') dx\right) \cdot \exp\left(-\int_0^{z'} \mu_e(x', z) dz\right), \quad (1)$$

$$I_2^1(x') = C_2 \cdot S \cdot I_0 \cdot \exp\left(-\int_0^{x'} \mu_e(x, z') dx\right) \cdot \underbrace{\exp\left(-\int_{z'}^L \mu_e(x', z) dz\right)}_A. \quad (2)$$

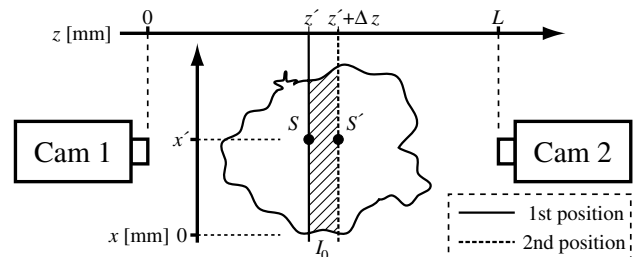


Fig. 1. Schematic of the detection arrangement for dual SLIPI. Two cameras, positioned at $\pm 90^\circ$, are used for the two SLIPI measurements. The dashed region between the two laser sheets indicate the probed volume over which the average extinction coefficient is calculated. The laser sheets propagate along the x direction.

Here the subscripts denote either camera, while the superscript indicates the recording number. S is a sample function defining the magnitude of the light scattered at 90° , and C describes the camera functions, such as collection angles and optics. The former of the two exponential terms in each equation describes the decay of the initial light intensity (laser extinction), while the latter is the reduction of the generated signal as it propagates toward the camera (signal attenuation). The laser beam is positioned at $z = z'$, while the two cameras are positioned at $z = 0$ or $z = L$, respectively. The beam is now shifted to $z = z' + \Delta z$, followed by an additional recording. The intensities reaching each camera are now expressed as

$$I_1^2(x') = C_1 \cdot S' \cdot I_0 \cdot \exp\left(-\int_0^{x'} \mu_e(x, z' + \Delta z) dx\right) \cdot \underbrace{\exp\left(-\int_0^{z'+\Delta z} \mu_e(x', z) dz\right)}_B, \quad (3)$$

$$I_2^2(x') = C_2 \cdot S' \cdot I_0 \cdot \exp\left(-\int_0^{x'} \mu_e(x, z' + \Delta z) dx\right) \cdot \exp\left(-\int_{z'+\Delta z}^L \mu_e(x', z) dz\right). \quad (4)$$

Because the laser sheet is shifted in space, the sample function is now denoted differently (to account for inhomogeneities). Rewriting terms A and B as the product of two exponential decays and dividing Eq. (1) with Eq. (2) as well as Eq. (3) with Eq. (4) leads to

$$\frac{I_1^1(x')}{I_2^1(x')} = \frac{C_1/C_2 \cdot \exp\left(-\int_0^{z'} \mu_e(x', z) dz\right)}{\exp\left(-\int_{z'+\Delta z}^{z'+\Delta z} \mu_e(x', z) dz\right) \cdot \exp\left(-\int_{z'+\Delta z}^L \mu_e(x', z) dz\right)}, \quad (5)$$

$$\frac{I_1^2(x')}{I_2^2(x')} = \frac{\exp\left(-\int_0^{z'} \mu_e(x', z) dz\right) \cdot \exp\left(-\int_{z'+\Delta z}^{z'+\Delta z} \mu_e(x', z) dz\right)}{C_2/C_1 \cdot \exp\left(-\int_{z'+\Delta z}^L \mu_e(x', z) dz\right)}. \quad (6)$$

Equations (5) and (6) contain parts with identical information that can be divided to unity, leaving only the exponential terms for the intensity decay between $z = z'$ and $z = z' + \Delta z$ according to

$$\frac{I_1^1(x') \cdot I_2^2(x')}{I_1^2(x') \cdot I_2^1(x')} = \exp\left(2 \int_{z'}^{z'+\Delta z} \mu_e(x', z) dz\right). \quad (7)$$

From this relation, the average extinction coefficient can now be calculated through Eq. (8):

$$\bar{\mu}_e(x') = \ln\left(\frac{I_1^1(x') \cdot I_2^2(x')}{I_1^2(x') \cdot I_2^1(x')}\right) \cdot \frac{1}{2\Delta z}. \quad (8)$$

In summation, the method can measure the average extinction coefficient between two locations, separated by Δz mm. Although explained only in one dimension, the method is capable of acquiring two-dimensional information, where the collection optics and number of pixels define the lateral resolution, while the axial is defined by Δz . The technique relies, however, on three assumptions. First, light scattering properties are assumed to be identical at $+90^\circ$ and -90° . According to the Mie theory, this is valid when probing spherical particles or random scattering media. Second, to perform pixel-to-pixel calculations, light is assumed to be collected at 90° only. A high camera f-number or spatial filtering is therefore appropriate. Finally, as the calculations are based on the Beer-Lambert law, only singly scattered photons should be detected. Multiply scattered light intensity present in the SLIPI images will lead to an underestimation of the extinction coefficients.

To investigate the axial resolution and to verify the technique, a cuvette filled with a homogeneous mixture of scattering polystyrene microspheres ($0.5 \mu\text{m}$ in diameter) and distilled water was probed. This provided prior knowledge, as the resulting extinction coefficients should be of a single value throughout the entire sample. Figure 2(a) shows an example of such a dual SLIPI measurement with $\Delta z = 4$ mm, together with images obtained using either laser sheet imaging or SLIPI. The graphs below each image show an average horizontal

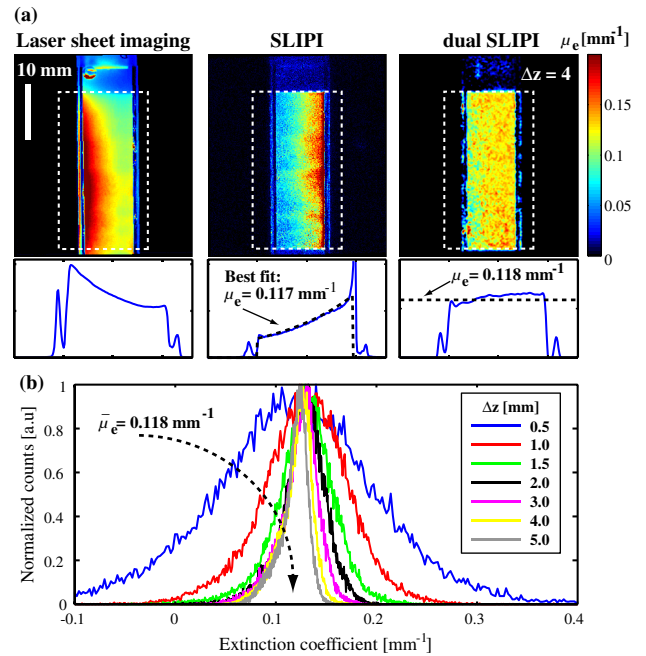


Fig. 2. (Color online) (a) Images and average cross sections of a homogeneous scattering sample obtained using laser sheet imaging, SLIPI and dual SLIPI with $\Delta z = 4$ mm. The laser sheet and SLIPI images are normalized to unity, whereas the extinction coefficient values are given by the color bar. (b) Histograms of the extinction coefficients for seven different Δz . It is seen that the results converge to a single value of μ_e , confirming the homogeneity of the probed sample.

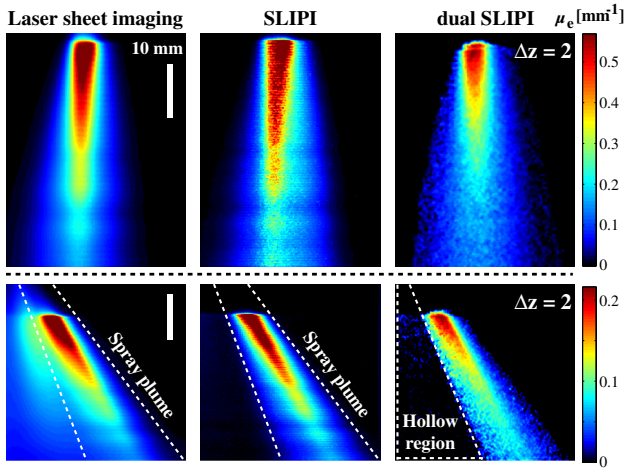


Fig. 3. (Color online) Images obtained using either laser sheet imaging, SLIPI, or dual SLIPI. Top row, solid cone spray. Bottom row, single-spray plume of a six-hole injector. The laser sheet and SLIPI images are normalized to unity, whereas the extinction coefficients are given in the color bar. Δz is given in millimeters. The laser sheet enters from the right.

cross section within the dashed area. The laser sheet image shows an increase of intensity with distance (the laser enters from the right), a consequence of detecting multiply scattered light. This falsely suggests that more particles are situated on the leftmost side. When suppressing multiply scattered light using SLIPI, the image shows an exponential decay of light intensity with distance, while the homogeneity can be seen directly with dual SLIPI. To evaluate these dual SLIPI results, the average extinction coefficient can also be estimated by fitting an exponential curve to the SLIPI data [see Fig. 2(a)]. The result $-\bar{\mu}_e = 0.117 \text{ mm}^{-1}$ is in accordance with the average value obtained with dual SLIPI ($\bar{\mu}_e = 0.118 \text{ mm}^{-1}$). Note that this alternative approach to extract μ_e is only applicable for homogeneous media.

Figure 2(b) shows histograms for seven dual SLIPI images of the cuvette, with Δz values ranging from 0.5 to 5 mm. As is shown, a too-small Δz (for this specific sample) results in a broadened histogram, with even negative values. However, all histograms converge to a single value $\bar{\mu}_e = 0.118 \text{ mm}^{-1}$ when increasing Δz , which indicate the homogeneity of the probed sample. These results demonstrate the trade-off between axial resolution and precision as the effect of signal attenuation over Δz must exceed the acquisition noise level.

Figure 3 shows a comparison between laser sheet imaging, SLIPI, and dual SLIPI when applied to inhomogeneous turbid media. Two different atomizing air-assisted water sprays were studied: one solid cone spray (top row) and one six-hole injector (bottom row). Because of the lack of specific spray structures (e.g., hollow regions) in the solid cone case, errors caused by multiply scattered light are not directly apparent. Applying SLIPI does not therefore lead to any distinct image

improvements but results in an asymmetric spray image. The dual SLIPI image does, however, reveal the true symmetry of the spray together with more accurate information regarding its inner conical structure. The six-hole injector consists of six spray plumes and, not too far downstream, a hollow central region. The three imaging techniques were applied on one of the plumes, and the images in Fig. 3 show approximately half of the spray. As seen, the hollow region becomes visible when multiply scattered light is suppressed using either SLIPI or dual SLIPI. Comparing the dual SLIPI results indicates that the solid cone spray is almost twice as dense, with values of μ_e up to $\sim 0.55 \text{ mm}^{-1}$. Also noticeable is that the dual SLIPI results are not affected by intensity variations in the laser sheet profile.

To conclude, dual SLIPI is a technique capable of acquiring depth-resolved images of the extinction coefficient. The method is based on side-scattering detection only, and because the sample is viewed from two opposite sides simultaneously, uncertainties related to the unknown distribution of scattering particles can be canceled out. This allows the technique to be applied on inhomogeneous media, given that three-way optical access is available. Multiply scattered light intensities, which lead to an underestimation of the extinction coefficient when detected, are suppressed by the implementation of SLIPI instead of traditional laser sheet imaging, thus improving both accuracy and precision. Finally, dual SLIPI does not require any calibration and can directly be applied to the central region of an inhomogeneous scattering medium.

Finally, the authors wish to thank the Linné Center within the Lund Laser Center as well as the Centre for Combustion Science and Technology through the Swedish Foundation for Strategic Research and the Swedish Energy Agency for financial support. Also the European Research Council Advanced Grant *Development and Application of Laser Diagnostic Techniques for Combustion Studies* is acknowledged.

References

1. L. Wang, X. Liang, P. Galland, P. P. Ho, and R. R. Alfano, *Opt. Lett.* **20**, 913 (1995).
2. A. Ansmann, M. Riebesell, and C. Weitkamp, *Opt. Lett.* **15**, 746 (1990).
3. H. Koh, D. Kim, S. Shin, and Y. Yoon, *Meas. Sci. Technol.* **17**, 2159 (2006).
4. J. Lim, Y. Sivathanu, V. Narayanan, and S. Chang, *Atomiz. Sprays* **13**, 27 (2003).
5. J. Huiskens, J. Swoger, F. Del Bene, J. Wittbrodt, and E. H. K. Stelzer, *Science* **305**, 1007 (2004).
6. E. Berrocal, E. Kristensson, M. Richter, M. Linne, and M. Aldén, *Opt. Express* **16**, 17870 (2008).
7. E. Kristensson, E. Berrocal, M. Richter, S. G. Pettersson, and M. Aldén, *Opt. Lett.* **33**, 2752 (2008).
8. M. A. A. Neil, R. Juškaitis, and T. Wilson, *Opt. Lett.* **22**, 1905 (1997).